Results in Optics 10 (2023) 100338

Contents lists available at ScienceDirect

Results in Optics

journal homepage: www.sciencedirect.com/journal/results-in-optics

Tunable cavity modes in diarylethene-based photo-switchable polymeric microcavities and study of the light-pulse propagation through the microcavities

Francesco Scotognella

Dipartimento di Fisica, Politecnico di Milano, Piazza Leonardo da Vinci 32, 20133 Milano, Italy

ARTICLE INFO

Keywords:
Tunable microcavity
Photochromic molecule
Light-pulse propagation
Transfer matrix method

ABSTRACT

Light responsive devices employing molecular photo-switches are interesting for displays and dynamic light filtering. In this work, polymeric microcavities embedding a layer of photochromic compound have been studied by means of the transfer matrix method. Different polymers, such as poly vinyl carbazole, poly styrene and cellulose acetate, have been used. A microcavity that includes random one-dimensional photonic structures sandwiching the photochromic layer has also been studied. Propagation of light pulses through the microcavities has been analysed.

1. Introduction

Photochromic materials are of great interest because of their employment in light-responsive devices, as for example rewritable displays, dynamic optical filters and optical memories (Torres-Pierna et al., 2020; Barachevsky, 2018; Naren et al., 2019; Castaing et al., 2021). In photochromism, an electromagnetic radiation-induced reversible transformation, from a thermodynamically more stable isomer A into a metastable isomer B, occurs (Boelke and Hecht, 2019). Recently, neuronal photo-stimulation has been demonstrated with an azobenzene-based photo-switch (DiFrancesco et al., 2020; Paternò et al., 2020).

The modulation of molecular photo-switches can be combined to the optical properties of photonic crystals, in order to achieve photo-modulation of the photonic band gap of the photonic crystal (Sridharan et al., 2010; Yagi et al., 2014). One-dimensional photonic crystals are very versatile systems that can be fabricated with several methods, such as spin coating (Scotognella et al., 2008; Scotognella et al., 2011; Pavlichenko et al., 2012; Manfredi et al., 2016), sputtering (Chiasera et al., 2015) and pulsed laser deposition (Natali et al., 2017; Nava et al., 2018), and that can be employed for sensors (Lotsch and Ozin, 2008; Georgiev et al., 2020; Aly and Mohamed, 2015; Aly and Mohamed, 2019; Awad and Aly, 2019; Aly et al., 2021b; Aly et al., 2021a; Al-Dossari et al., 2022; Aly et al., 2022; Zaky et al., 2022; Aly et al., 2017) and lasers (Lei et al., 1991; Komikado et al., 2006; Scotognella et al., 2011). A one-dimensional microcavity can be obtained by placing a defect layer between two one-dimensional photonic crystals (Takeuchi et al., 2007; Frezza et al., 2011; Aly et al., 2020). Microcavities that include photochromic materials have been reported in pioneering works (Knarr et al., 2016; Lova et al., 2018).

In this work, it is proposed for the first time a defect layer of the molecular photo-switch diarylethene1 (Irie and Morimoto, 2009; Morimoto et al., 2017) that has been embedded between two polymeric one-dimensional photonic crystals, made alternating either poly vinyl carbazole and poly styrene or poly vinyl carbazole and cellulose acetate. A microcavity, in which the defect includes random photonic crystals that embed the diarylethene1 layer, is also studied. The optical properties of the microcavities have been simulated via the transfer matrix method, considering the refractive index dispersions of all the materials. The photo-stimulation of diarylethene1 leads to a modulation of the cavity modes. The transmission of a light pulse through the microcavities has been studied, highlighting a temporal delay in correspondence of the cavity modes.

2. Methods

The transfer matrix method is a powerful tool to describe the optical properties of the one-dimensional photonic structures (Born et al., 1999; Boucher et al., 2009; Xiao et al., 2016; Aly et al., 2009; Ahmed and Mehaney, 2021; Wu and Gao, 2021; Aly et al., 2020). The studied system is glass/multilayer/air with light that impinges the sample orthogonally with respect to the sample surface (in this configuration, the transmission spectra for TE and TM waves are the same (Bellingeri et al.,

E-mail address: francesco.scotognella@polimi.it.

https://doi.org/10.1016/j.rio.2022.100338
Received 26 October 2022; Received in revised form 29 November 2022; Accepted 4 December 2022
Available online 5 December 2022

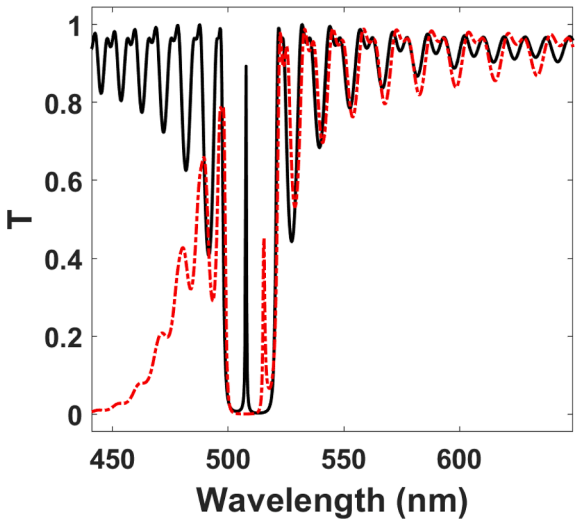

Fig. 1. Transmission spectra of the microcavity $(PVK/PS)_{40}$/diarylethene1/$(PS/PVK)_{40}$ with diarylethene1 in the open form (solid black curve) and in the closed form (dashed red curve)

2017). Within this framework the parameter

$$\phi_k(\lambda) = \frac{2\pi}{\lambda} n_k(\lambda) d_k \tag{1}$$

is used the characteristic matrix for the kth layer (Born et al., 1999)

$$M_k = \begin{bmatrix} cos\phi_k(\lambda) & -\frac{i}{n_k(\lambda)} sin\phi_k(\lambda) \\ -in_k(\lambda) sin\phi_k(\lambda) & cos\phi_k(\lambda) \end{bmatrix} \tag{2}$$

with $n_k(\lambda)$ and d_k the wavelength-dependent refractive index and the thickness (in nm), respectively, of the kth layer. The matrix for the multilayer is given by

$$M = \begin{bmatrix} M_{11} & M_{12} \\ M_{21} & M_{22} \end{bmatrix} = \prod_{i=1}^{N} M_k \tag{3}$$

With N the number of layers. From the matrix M it is possible to determine the transmission coefficient t:

$$t = \frac{2n_s}{(M_{11} + M_{12}n_0)n_s + (M_{21} + M_{22}n_0)} \tag{4}$$

And the transmission T:

$$T = \frac{n_0}{n_s}|t|^2 \tag{5}$$

n_s and n_0 are the refractive indexes of the substrate (glass, $n_s = 1.46$) and air, respectively.

The transmission spectra of the multilayer structures have been studied in the spectra range between 440 nm and 650 nm.

The temporal response of the systems has been studied by employing the inverse fast Fourier transform of the product of the incoming light pulse and the transmission spectrum of the multilayers. The transmitted time resolved signal $T(t)$ can be written as

$$T(t) = \mathscr{F}^{-1}[G(\omega)T(\omega)] = \int_{-\infty}^{\infty} G(\omega)T(\omega)e^{i\omega t}d\omega \tag{6}$$

In which $G(\omega)$ is the Gaussian spectral profile of the incoming light pulse and $T(\omega)$ is the transmission spectrum of the multilayers (Ghulinyan et al., 2005).

The multilayers are made with different materials, such as diarylethene1 (Morimoto et al., 2017), poly vinyl carbazole (PVK), poly styrene (PS), cellulose acetate (CA). The complex refractive index of diarylethene1, in its open and close form, is reported in Ref. (Scotognella, 2020). The Sellmeier equations can be employed in the simulations to describe the refractive index dispersion of the materials employed (Natesan et al., 2019; Amiri et al., 2019). The Sellmeier equation for the refractive index of PVK is given by (Manfredi et al., 2016; Fornasari et al., 2016):

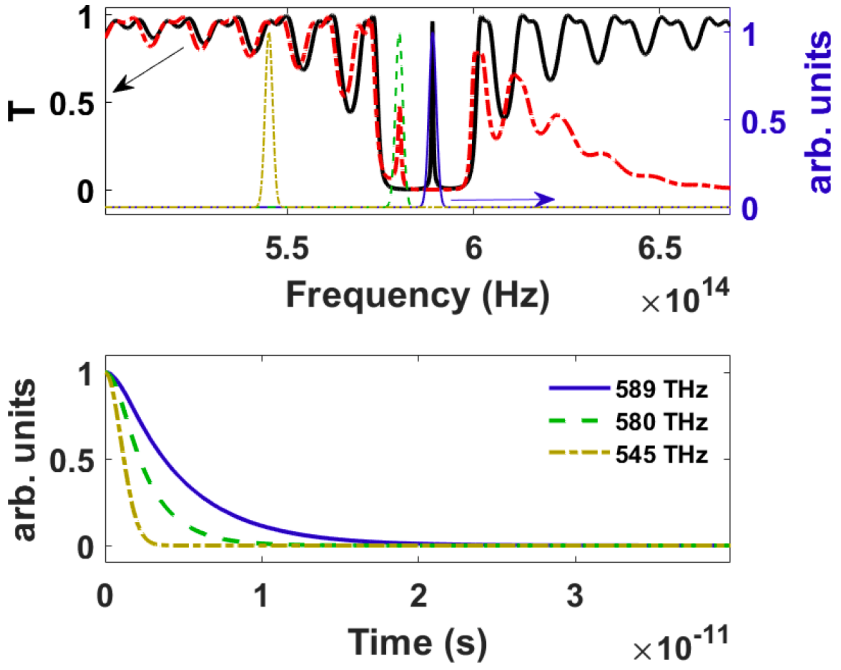

Fig. 2. (above) Transmission spectra of the microcavity $(PVK/PS)_{40}$/diarylethene1/$(PS/PVK)_{40}$, with diarylethene1 in the open form (solid black curve) and in the closed form (dashed red curve), and spectral shapes of three light pulses centred at 545, 580 and 589 THz. (below) Time-resolved transmitted signals through the microcavity.

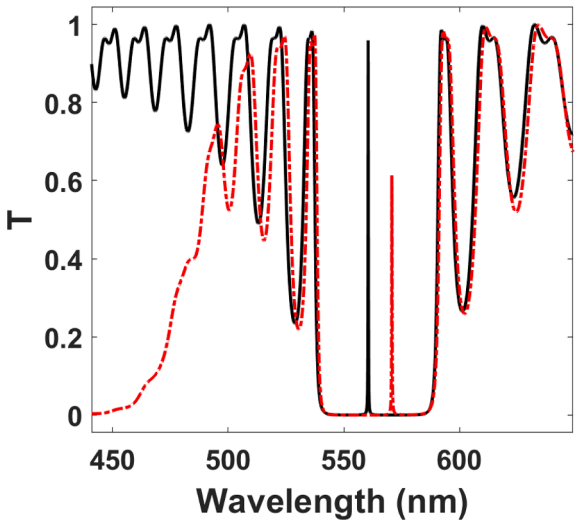

Fig. 3. Transmission spectra of the microcavity $(PVK/CA)_{25}$/diarylethene1/$(PS/PVK)_{25}$ with diarylethene1 in the open form (solid black curve) and in the closed form (dashed red curve).

$$n^2_{PVK}(\lambda) - 1 = \frac{0.09788\lambda^2}{\lambda^2 - 0.3257^2} + \frac{0.6901\lambda^2}{\lambda^2 - 0.1419^2} + \frac{0.8513\lambda^2}{\lambda^2 - 1.1417^2} \quad (7)$$

The Sellier equation for the refractive index of PS is given by (RefractiveIndex.INFO, 2019; Sultanova et al., 2009):

$$n^2_{PS}(\lambda) - 1 = \frac{1.4435\lambda^2}{\lambda^2 - 0.020216^2} \quad (8)$$

Finally, the Sellmeier equation for the refractive index of CA is (Manfredi et al., 2016; Fornasari et al., 2016):

$$n^2_{CA}(\lambda) - 1 = \frac{0.6481\lambda^2}{\lambda^2 - 0.0365^2} + \frac{0.5224\lambda^2}{\lambda^2 - 0.1367^2} + \frac{2.483\lambda^2}{\lambda^2 - 13.54^2} \quad (9)$$

In the Sellemeier equations λ is in micrometers.

3. Results and discussion

In this work different microcavities that embed a diarylethene1 layer between two polymeric one-dimensional photonic crystals are studied. The one-dimensional photonic crystals are made by alternating either layers of PVK and PS or layers of PVK and CA. Moreover, it has been studied a microcavity in which the defect is made by the diarylethene layer sandwiched by two random photonic crystal of 20 layers of PVK and PS; the defect is embedded between two one-dimensional photonic crystals of PVK and CA.

The first microcavity is made with a diarylethene1 defect layer between two photonic crystals of 40 bilayers of PVK and PS (for a total of 161 layers). Thus, the studied system is glass/$(PVK/PS)_{40}$/

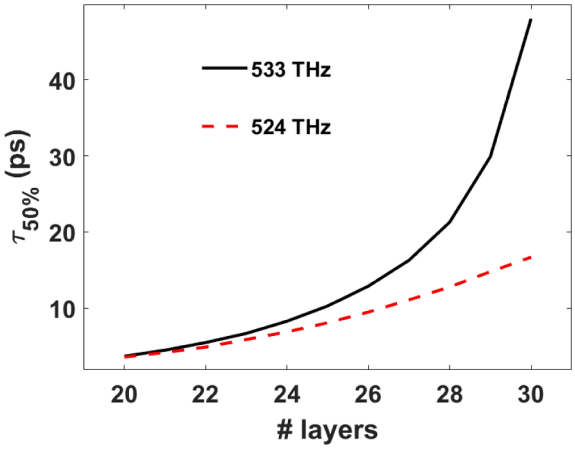

Fig. 5. Delay time of the transmitted light pulses through the $(PVK/CA)_{NL}$/diarylethene1/$(CA/PVK)_{NL}$ microcavity, corresponding to 50% of the intensity of the initial signal, as a function of the number of layers *NL* (black solid curve is related to diarylethene1 in the open form, red dashed curve is related to diarylethene1 in the closed form).

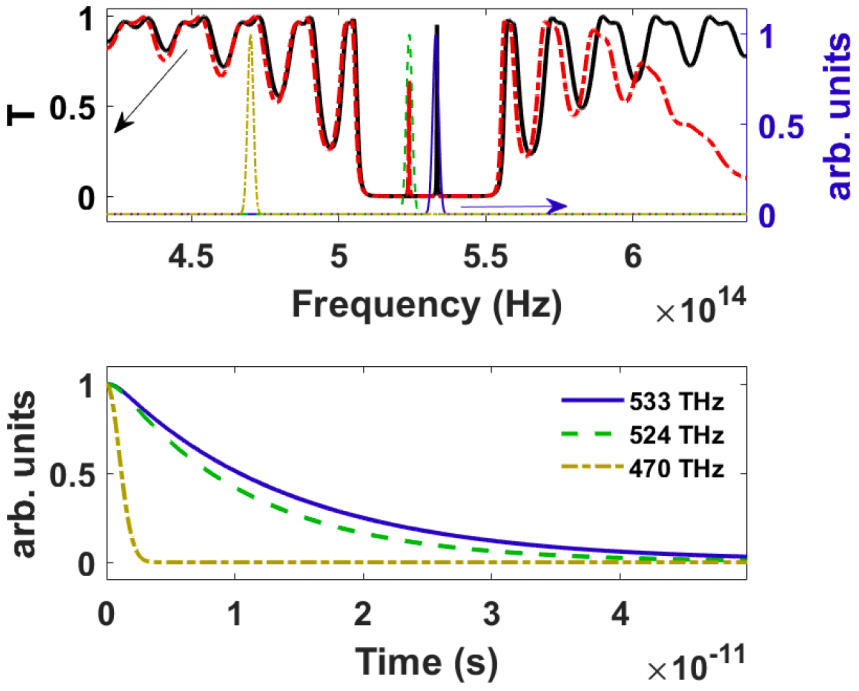

Fig. 4. (above) Transmission spectra of the microcavity $(PVK/CA)_{25}$/diarylethene1/$(CA/PVK)_{25}$, with diarylethene1 in the open form (solid black curve) and in the closed form (dashed red curve), and spectral shapes of three light pulses centred at 470, 524 and 533 THz. (below) Time-resolved transmitted signals through the microcavity.

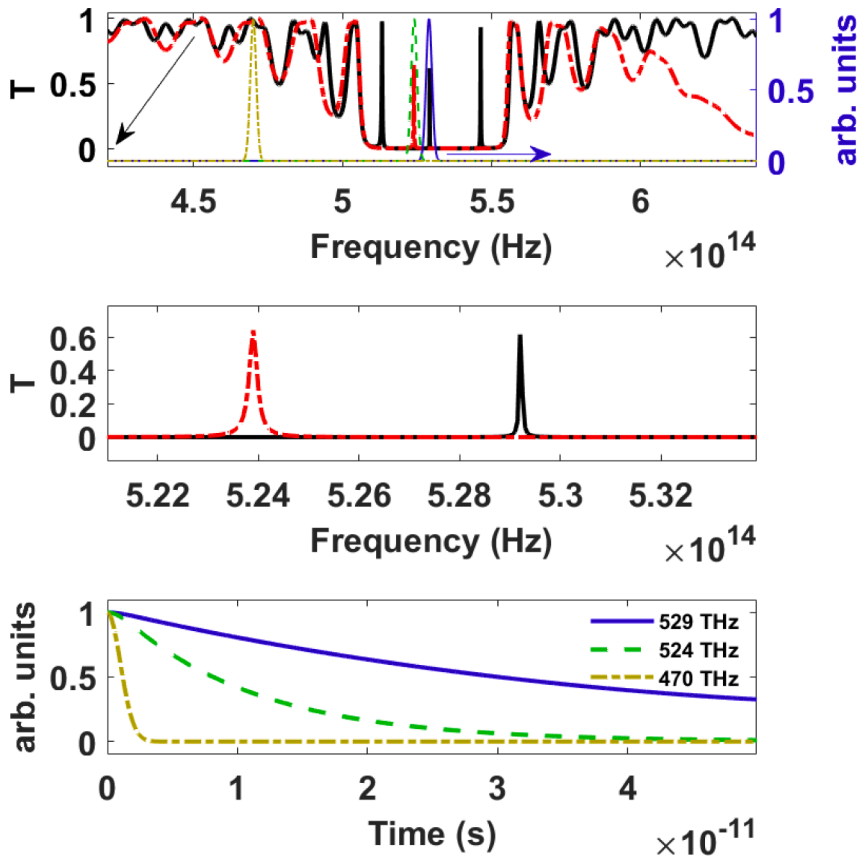

Fig. 6. (above) Transmission spectra of the microcavity $(PVK/CA)_{25}$/(randomPVK/PS)/diarylethene1/(randomPVK/PS)/$(CA/PVK)_{25}$, with diarylethene1 in the open form (solid black curve) and in the closed form (dashed red curve), and spectral shapes of three light pulses centred at 470, 524 and 529 THz. (middle) Magnification of the transmission spectrum in the region of the central cavity modes. (below) Time-resolved transmitted signals through the microcavity.

diarylethene1/$(PS/PVK)_{40}$/air. The thickness of the PVK layers is 75.2 nm, the thickness of the PS layers is 79.9 nm, and the thickness of diarylethene1 defect layer is 150.4 nm. In Fig. 1 the transmission spectra of the microcavity $(PVK/PS)_{40}$/diarylethene1/$(PS/PVK)_{40}$ with diarylethene1 in the open form (solid black curve) and in the closed form (dashed red curve) are shown.

With the photo-stimulation the complex refractive index of diarylethene1 is changing, inducing a shift of the cavity mode in the microcavity. In Fig. 2 (above) the transmission spectra of the microcavity $(PVK/PS)_{40}$/diarylethene1/$(PS/PVK)_{40}$, with diarylethene1 in the open form (solid black curve) and in the closed form (dashed red curve) are shown together with the spectral shapes of three light pulses centred at 545, 580 and 589 THz. The width of the (Gaussian) peaks is 1 THz. With equation (6) the time-resolved transmitted signals through the microcavity (Fig. 2, below). The duration of the pulse out of the cavity (545 THz) is 1 picosecond, while the pulses at 580 THz (for Diarylethene1 in the open form) and at 589 THz (for Diarylethene1 in the closed form) are significantly delayed.

The second studied system is glass/$(PVK/CA)_{25}$/diarylethene1/$(CA/PVK)_{25}$/air. The thickness of the PVK layers is 84 nm, the thickness of the CA layers is 95.2 nm, and the thickness of diarylethene1 defect layer is 172.8 nm. In Fig. 3 the transmission spectra of the microcavity $(PVK/CA)_{25}$/diarylethene1/$(PS/PVK)_{25}$ (for a total of 101 layers) with diarylethene1 in the open form (solid black curve) and in the closed form (dashed red curve) are shown. With respect to the microcavity with PVK and PS the chosen number of bilayers of the two photonic crystals is smaller. Nevertheless, the transmission in the photonic band region is close to zero in both microstructures. This is due to refractive index contrast, which is higher in the case of PVK and CA (at about 600 nm, $\Delta n_{PVK-CA} = n_{PVK} - n_{CA} \cong 0.183$, $\Delta n_{PVK-PS} = n_{PVK} - n_{PS} \cong 0.074$, respectively).

In Fig. 4 (above) the transmission of the microcavity is reported together with the spectral shapes of three light pulses at 470, 524 and 533 THz. As in the microcavity with PVK and PS, the light pulses in correspondence of the cavity modes, for diarylethene1 in the open and closed forms, are delayed (Fig. 4, below).

The delay time of the two pulses can be tuned by varying the number of the layers in the microcavity. In Fig. 5 the delay time of the transmitted light pulses through the $(PVK/CA)_{NL}$/diarylethene1/$(CA/PVK)_{NL}$ microcavity, corresponding to 50 % of the intensity of the initial signal, as a function of the number of layers *NL* is shown.

In the third microcavity the defect layer includes two PVK/PS random photonic sequences of 20 layers, sandwiching the diarylethene1 layer. The defect is embedded between two PVK/CA one-dimensional photonic crystals. Thus, the structure of the microcavity is $(PVK/CA)_{25}$/PVK/PS/PS/PS/PVK/PS/PS/PVK/PS/PVK/PS/PVK/PS/PVK/PS/PVK/PVK/PVK/PVK/PS/diarylethene1/PVK/PS/PS/PS/PS/PVK/PS/PS/PS/PS/PS/PVK/PS/PVK/PVK/PVK/PS/PS/PVK/PVK/$(CA/PVK)_{25}$ (for a total of 141 layers). The thickness of the PVK layers is 84 nm, the thickness of the PS layers is 89.6 nm, the thickness of the CA layers is 95.2 nm, and the thickness of diarylethene1 defect layer is 172.8 nm.

The delay time for the transmitted signals at 529 THz, for the microcavity with diarylethene1 in the open form, and at 524 THz, for the microcavity with diarylethene1 in the closed form, is significantly different. This is due to the fact that the disorder in the microcavity leads to a broader cavity mode in the case of diarylethene1 in the closed form (dashed red curve in Fig. 6, middle).

With the PVK/PS microcavity a shift, from the cavity mode for diarylethene1 in the open form to the one with the dye in the closed form,

related to $\Delta\lambda/\lambda = 0.015$ has been achieved, while with the PVK/CA microcavity a shift related to $\Delta\lambda/\lambda = 0.018$ has been achieved. With the PVK/CA random sequence microcavity, the shift corresponds to a $\Delta\lambda/\lambda = 0.010$. In literature, experiments on $(PVK/CA)_{15}/PVA/PMA4/PVA/(CA/PVK)_{15}$ report a $\Delta\lambda/\lambda = 0.011$ (Knarr et al., 2016; Lova et al., 2018).

The microcavities studied in this work are made of layers of polymers. In the usual fabrication procedure of these layers, such layers are baked at 80 °C (Komikado et al., 2006). For this reason, it is recommended to employ such microcavities at temperatures below 80 °C.

4. Conclusion

In this study different microcavities in which a diarylethene1 layer is sandwiched between two polymeric one-dimensional photonic crystals have been simulated for the first time by means of the transfer matrix method. The one-dimensional photonic crystals have been designed by alternating either layers of PVK and PS or layers of PVK and CA. Furthermore, it has been analysed a microcavity in which the defect layer of diarylethene1 is sandwiched between two random photonic crystals of 50 layers of PVK and PS. In such microcavity the defect (of 81 layers in total) is embedded between two one-dimensional photonic crystals of PVK and CA. Light pulse propagation through these microcavities have been also analysed, highlighting a modulation of the light pulse delay out of the cavity band gap and in the cavity modes with diarylethene1 in the open and closed forms. The microcavities designed in this work can be experimentally fabricated with low cost techniques, such as spin coating (Takeuchi et al., 2007; Knarr et al., 2016; Komikado et al., 2006). The microcavities presented in this work show defect mode shifts that are comparable with microcavities reported in literature with another photochromic material, i.e. PMA4 (Knarr et al., 2016; Lova et al., 2018). Such findings can be interesting for the fabrication of dynamic light filters via tunable structural colour and optical memories.

Declaration of Competing Interest

The authors declare that they have no known competing financial interests or personal relationships that could have appeared to influence the work reported in this paper.

Data availability

Data will be made available on request.

Acknowledgement

This work was supported by Grant No. CFPMN1–008 from the Department of National Defence Discovery supplement and IDEAS.

References

Ahmed, A.M., Mehaney, A., 2021. Novel design of wide temperature ranges sensor based on Tamm state in a pyroelectric photonic crystal with high sensitivity. Physica E 125, 114387. https://doi.org/10.1016/j.physe.2020.114387.

Al-Dossari, M., Awasthi, S.K., Mohamed, A.M., Abd El-Gawaad, N.S., Sabra, W., Aly, A. H., 2022. Bio-Alcohol Sensor Based on One-Dimensional Photonic Crystals for Detection of Organic Materials in Wastewater. Materials 15, 4012. https://doi.org/10.3390/ma15114012.

Aly, A.H., Mohamed, D., 2015. BSCCO/SrTiO3 One Dimensional Superconducting Photonic Crystal for Many Applications. J. Supercond. Nov. Magn. 28, 1699–1703. https://doi.org/10.1007/s10948-015-2993-x.

Aly, A.H., Mohamed, D., 2019. The Optical Properties of Metamaterial-Superconductor Photonic Band Gap With/Without Defect Layer. J. Supercond. Nov. Magn. 32, 1897–1902. https://doi.org/10.1007/s10948-018-4922-2.

Aly, A.H., Ryu, S.-W., Hsu, H.-T., Wu, C.-J., 2009. THz transmittance in one-dimensional superconducting nanomaterial-dielectric superlattice. Mater. Chem. Phys. 113, 382–384. https://doi.org/10.1016/j.matchemphys.2008.07.123.

Aly, A.H., Sabra, W., Elsayed, H.A., 2017. Cutoff frequency in metamaterials photonic crystals within Terahertz frequencies. Int. J. Mod. Phys. B 31, 1750123. https://doi.org/10.1142/S0217979217501235.

Aly, A.H., Ghany, S.-E.-S.-A., Kamal, B.M., Vigneswaran, D., 2020. Theoretical studies of hybrid multifunctional YaBa2Cu3O7 photonic crystals within visible and infra-red regions. Ceram. Int. 46, 365–369. https://doi.org/10.1016/j.ceramint.2019.08.270.

Aly, A.H., Mohamed, D., Mohaseb, M.A., 2020. Metamaterial Control of Hybrid Multifunctional High-Tc Superconducting Photonic Crystals for 1D Quasi-periodic Structure Potential Applications. Mat. Res. 23, e20190695.

Aly, A.H., Awasthi, S.K., Mohamed, A.M., Al-Dossari, M., Matar, Z.S., Mohaseb, M.A., et al., 2021a. 1D reconfigurable bistable photonic device composed of phase change material for detection of reproductive female hormones. Phys. Scr. 96, 125533 https://doi.org/10.1088/1402-4896/ac3efa.

Aly, A.H., Ameen, A.A., Mahmoud, M.A., Matar, Z.S., Al-Dossari, M., Elsayed, H.A., 2021b. Photonic Crystal Enhanced by Metamaterial for Measuring Electric Permittivity in GHz Range. Photonics 8, 416. https://doi.org/10.3390/photonics8100416.

Aly, A.H., Awasthi, S.K., Mohaseb, M.A., Matar, Z.S., Amin, A.F., 2022. MATLAB Simulation-Based Theoretical Study for Detection of a Wide Range of Pathogens Using 1D Defective Photonic Structure. Crystals 12, 220. https://doi.org/10.3390/cryst12020220.

Amiri, I.S., Paul, B.K., Ahmed, K., Aly, A.H., Zakaria, R., Yupapin, P., et al., 2019. Tri-core photonic crystal fiber based refractive index dual sensor for salinity and temperature detection. Microw. Opt. Technol. Lett. 61, 847–852. https://doi.org/10.1002/mop.31612.

Awad, M.A., Aly, A.H., 2019. Experimental and theoretical studies of hybrid multifunctional TiO2/TiN/TiO2. Ceram. Int. 45, 19036–19043. https://doi.org/10.1016/j.ceramint.2019.06.145.

Barachevsky, V.A., 2018. Advances in photonics of organic photochromism. J. Photochem. Photobiol. A Chem. 354, 61–69. https://doi.org/10.1016/j.jphotochem.2017.06.034.

Bellingeri, M., Chiasera, A., Kriegel, I., Scotognella, F., 2017. Optical properties of periodic, quasi-periodic, and disordered one-dimensional photonic structures. Opt. Mater. 72, 403–421. https://doi.org/10.1016/j.optmat.2017.06.033.

Boelke, J., Hecht, S., 2019. Designing Molecular Photoswitches for Soft Materials Applications. Adv. Opt. Mater. 7, 1900404. https://doi.org/10.1002/adom.201900404.

Born, M., Wolf, E., Bhatia, A.B., Clemmow, P.C., Gabor, D., Stokes, A.R., et al., 1999. In: Principles of Optics: Electromagnetic Theory of Propagation, Interference and Diffraction of Light, 7th ed. Cambridge University Press. https://doi.org/10.1017/CBO9781139644181.

Boucher, Y.G., Chiasera, A., Ferrari, M., Righini, G.C., 2009. Extended transfer matrix modeling of an erbium-doped cavity with SiO2/TiO2 Bragg reflectors. Opt. Mater. 31, 1306–1309. https://doi.org/10.1016/j.optmat.2008.10.028.

Castaing, V., Giordano, L., Richard, C., Gourier, D., Allix, M., Viana, B., 2021. Photochromism and Persistent Luminescence in Ni-Doped ZnGa2O4 Transparent Glass-Ceramics: Toward Optical Memory Applications. J. Phys. Chem. C 125, 10110–10120. https://doi.org/10.1021/acs.jpcc.1c01900.

Chiasera, A., Scotognella, F., Criante, L., Varas, S., Valle, G.D., Ramponi, R., et al., 2015. Disorder in Photonic Structures Induced by Random Layer Thickness. Sci. Adv. Mater. 7, 1207–1212. https://doi.org/10.1166/sam.2015.2249.

DiFrancesco, M.L., Lodola, F., Colombo, E., Maragliano, L., Bramini, M., Paternò, G.M., et al., 2020. Neuronal firing modulation by a membrane-targeted photoswitch. Nat. Nanotechnol. 15, 296–306. https://doi.org/10.1038/s41565-019-0632-6.

Fornasari, L., Floris, F., Patrini, M., Comoretto, D., Marabelli, F., 2016. Demonstration of fluorescence enhancement via Bloch surface waves in all-polymer multilayer structures. Phys. Chem. Chem. Phys. 18, 14086–14093. https://doi.org/10.1039/C5CP07660A.

Frezza, L., Patrini, M., Liscidini, M., Comoretto, D., 2011. Directional Enhancement of Spontaneous Emission in Polymer Flexible Microcavities. J. Phys. Chem. C 115, 19939–19946. https://doi.org/10.1021/jp206105r.

Georgiev, R., Lazarova, K., Vasileva, M., Babeva, T., 2020. All niobia Bragg stacks for optical sensing of vapors. Opt. Quant. Electron. 52, 114. https://doi.org/10.1007/s11082-020-2243-8.

Ghulinyan, M., Oton, C.J., Dal Negro, L., Pavesi, L., Sapienza, R., Colocci, M., et al., 2005. Light-pulse propagation in Fibonacci quasicrystals. Phys. Rev. B 71, 094204. https://doi.org/10.1103/PhysRevB.71.094204.

Irie, M., Morimoto, M., 2009. Photochromic diarylethene molecules and crystals. Pure Appl. Chem. 81, 1655–1665. https://doi.org/10.1351/PAC-CON-08-09-26.

Knarr, R.J., Manfredi, G., Martinelli, E., Pannocchia, M., Repetto, D., Mennucci, C., et al., 2016. In-plane anisotropic photoresponse in all-polymer planar microcavities. Polymer 84, 383–390. https://doi.org/10.1016/j.polymer.2016.01.009.

Komikado, T., Yoshida, S., Umegaki, S., 2006. Surface-emitting distributed-feedback dye laser of a polymeric multilayer fabricated by spin coating. Appl. Phys. Lett. 89, 061123 https://doi.org/10.1063/1.2336740.

Lei, C., Rogers, T.J., Deppe, D.G., Streetman, B.G., 1991. ZnSe/CaF2 quarter-wave Bragg reflector for the vertical-cavity surface-emitting laser. J. Appl. Phys. 69, 7430–7434. https://doi.org/10.1063/1.347557.

Lotsch, B.V., Ozin, G.A., 2008. Clay Bragg Stack Optical Sensors. Adv. Mater. 20, 4079–4084. https://doi.org/10.1002/adma.200800914.

Lova, P., Manfredi, G., Comoretto, D., 2018. Advances in Functional Solution Processed Planar 1D Photonic Crystals. Adv. Opt. Mater. 6, 1800730. https://doi.org/10.1002/adom.201800730.

Manfredi, G., Mayrhofer, C., Kothleitner, G., Schennach, R., Comoretto, D., 2016. Cellulose ternary photonic crystal created by solution processing. Cellul. 23, 2853–2862. https://doi.org/10.1007/s10570-016-1031-x.

Morimoto, M., Sumi, T., Irie, M., 2017. Photoswitchable Fluorescent Diarylethene Derivatives with Thiophene 1,1-Dioxide Groups: Effect of Alkyl Substituents at the Reactive Carbons. Materials 10, 1021. https://doi.org/10.3390/ma10091021.

Naren, G., Hsu, C.-W., Li, S., Morimoto, M., Tang, S., Hernando, J., et al., 2019. An all-photonic full color RGB system based on molecular photoswitches. Nat. Commun. 10, 3996. https://doi.org/10.1038/s41467-019-11885-4.

Natali, M., Quiroga, S.D., Passoni, L., Criante, L., Benvenuti, E., Bolognini, G., et al., 2017. Simultaneous Tenfold Brightness Enhancement and Emitted-Light Spectral Tunability in Transparent Ambipolar Organic Light-Emitting Transistor by Integration of High-k Photonic Crystal. Adv. Funct. Mater. 27, 1605164. https://doi.org/10.1002/adfm.201605164.

Natesan, A., Govindasamy, K.P., Gopal, T.R., Dhasarathan, V., Aly, A.H., 2019. Tricore photonic crystal fibre based refractive index sensor for glucose detection. IET Optoelectron. 13, 118–123. https://doi.org/10.1049/iet-opt.2018.5079.

Nava, G., Fumagalli, F., Neutzner, S., Fonzo, F.D., 2018. Large area porous 1D photonic crystals comprising silicon hierarchical nanostructures grown by plasma-assisted, nanoparticle jet deposition. Nanotechnology 29, 465603. https://doi.org/10.1088/1361-6528/aade21.

Paternò, G.M., Colombo, E., Vurro, V., Lodola, F., Cimò, S., Sesti, V., et al., 2020. Membrane Environment Enables Ultrafast Isomerization of Amphiphilic Azobenzene. Adv. Sci. 7, 1903241. https://doi.org/10.1002/advs.201903241.

Pavlichenko, I., Exner, A.T., Guehl, M., Lugli, P., Scarpa, G., Lotsch, B.V., 2012. Humidity-Enhanced Thermally Tunable TiO2/SiO2 Bragg Stacks. J. Phys. Chem. C 116, 298–305. https://doi.org/10.1021/jp208733t.

RefractiveIndex.INFO - Refractive index database n.d. https://refractiveindex.info/ (accessed November 15, 2019).

Scotognella, F., 2020. Multilayer plasmonic photonic structures embedding photochromic molecules or optical gain molecules. Physica E 114081. https://doi.org/10.1016/j.physe.2020.114081.

Scotognella, F., Monguzzi, A., Cucini, M., Meinardi, F., Comoretto, D., Tubino, R., 2008. One Dimensional Polymeric Organic Photonic Crystals for DFB Lasers. Int. J. Photoenergy. https://doi.org/10.1155/2008/389034.

Scotognella, F., Puzzo, D.P., Zavelani-Rossi, M., Clark, J., Sebastian, M., Ozin, G.A., et al., 2011. Two-Photon Poly(phenylenevinylene) DFB Laser. Chem. Mater. 23, 805–809. https://doi.org/10.1021/cm102102w.

Sridharan, D., Waks, E., Solomon, G., Fourkas, J.T., 2010. Reversible tuning of photonic crystal cavities using photochromic thin films. Appl. Phys. Lett. 96, 153303 https://doi.org/10.1063/1.3377910.

Sultanova, N., Kasarova, S., Nikolov, I., 2009. Dispersion Properties of Optical Polymers. Acta Phys. Pol. A 116, 585–587. https://doi.org/10.12693/APhysPolA.116.585.

Takeuchi, H., Natsume, K., Suzuki, S., Sakata, H., 2007. Microcavity distributed-feedback laser using dye-doped polymeric thin films. Electron. Lett. 43, 30–31. https://doi.org/10.1049/el:20073399.

Torres-Pierna, H., Ruiz-Molina, D., Roscini, C., 2020. Highly transparent photochromic films with a tunable and fast solution-like response. Mater. Horiz. 7, 2749–2759. https://doi.org/10.1039/D0MH01073A.

Wu, J., Gao, J., 2021. Multi-band absorption characteristics of a metal-loaded graphene-based photonic crystal. Physica E 129, 114675. https://doi.org/10.1016/j.physe.2021.114675.

Xiao, X., Wenjun, W., Shuhong, L., Wanquan, Z., Dong, Z., Qianqian, D., et al., 2016. Investigation of defect modes with Al2O3 and TiO2 in one-dimensional photonic crystals. Optik 127, 135–138. https://doi.org/10.1016/j.ijleo.2015.10.005.

Yagi, R., Katae, H., Kuwahara, Y., Kim, S.-N., Ogata, T., Kurihara, S., 2014. On-off switching properties of one-dimensional photonic crystals consisting of azo-functionalized polymer liquid crystals having different methylene spacers and polyvinyl alcohol. Polymer 55, 1120–1127. https://doi.org/10.1016/j.polymer.2014.01.018.

Zaky, Z.A., Panda, A., Pukhrambam, P.D., Aly, A.H., 2022. The impact of magnetized cold plasma and its various properties in sensing applications. Sci. Rep. 12, 3754. https://doi.org/10.1038/s41598-022-07461-4.